D. Fabiani and G. C. Montanari

The effect of voltage distortion on ageing acceleration of insulation systems under partial discharge activity

in IEEE Electrical Insulation Magazine, vol. 17, no. 3, pp. 24-33, May-June 2001.

THE EFFECT OF VOLTAGE DISTORTION ON AGING ACCELERATION OF INSULATION SYSTEMS UNDER PARTIAL DISCHARGE ACTIVITY

D. Fabiani G. C. Montanari
Laboratorio di Ingegneria dei Materiali ed Alta Tensione (LIMAT)
Dipartimento di Ingegneria Elettrica
University of Bologna
Viale Risorgimento, 2 – 40136 Bologna

Keywords: Power converters, Harmonics, Multistress, Insulation reliability, Life models

1 Introduction

Power electronic equipments are the main responsible for harmonic pollution of AC-electrical plants. In particular, Adjustable Speed Drives (ASD) affect both the AC-supply network and electrical motor supply voltage. A significant reliability reduction of equipment insulation fed by distorted voltage waveforms has been observed since 1950, but only recently voltage distortion effects on insulation have been deeply investigated. However, it is doubtful that the limit for power quality fixed by IEEE and IEC standards [1-3], which regard voltage and current rms distortion, can really improve electrical insulation reliability. Mostly, emphasis is put on current distortion, since accelerated aging is related to overheating caused by power loss increase [4-8]. Only recently the effect of voltage distortion on insulation system performance has been highlighted [9-12], focusing on cables and capacitors.

Historically, investigations of the effect of voltage and current distortion on insulation degradation started from the harmonics injected in the AC distribution network by distorting loads [13]**,** typically low-order harmonics (from 3^{rd} to 21^{st} order, i.e. having frequency from 3 to 21 times the fundamental one). Most of the work of the previous decade, in fact, was referred to transformers, rotating machines, cables and capacitors subjected to supply voltage distortion [5, 6].

The recent large diffusion of Adjustable Speed Drives (ASD) has brought significant attention to another possible cause of loss of insulation reliability, i.e. the steep waveforms generated by AC/AC converters using fast electronic switches (as MOS-FET or IGBT), e.g. [14-23]. These inverters generate width-modulated pulse trains with very high slew rate (up to 50 kV/us) and frequency (10-50 kHz). Electrical machines with insulation designed for supply frequency (50-60 Hz) have shown premature breakdown due to these periodic supply pulses, so that work is being

carried out to envisage design solutions including e.g. filters, winding techniques, new materials. In particular the endurance of the so-called “corona resistant” materials, i.e. materials resisting to Partial Discharge (PD) activity at high frequency, is being investigated [14-25].

This paper focuses on the features of harmonic distortion which may affect significantly reliability of typical AC-power network equipments, such as low-voltage self-healing capacitors used for reactive power and harmonic compensation. Moreover, the effect of high-frequency pulse-like voltage generated by ASD on electrical machine insulation is also investigated, resorting to life tests carried out on different insulating materials of the standard and “corona resistant” type, at electrical field levels able to incept partial discharges (PD).

2 Harmonic distortion and insulation systems

Electronic power converters (AC/DC, DC/AC) are the main responsible for voltage and current distortion in electrical networks [6, 7]. These converters are now frequently employed also in electrical machine speed control, so that harmonic distortion can affect motor winding insulation.

An example of a simple electrical network is sketched in Fig. 1: an ASD (Adjustable Speed Drive) is the polluting load, composed by an AC/DC converter, DC-bus-filter and DC/AC inverter; Z_l is the supply line equivalent impedance. A capacitor bank for reactive power compensation, C_K, and non-distorting loads are also connected to the network busbar; Z_C is the equivalent impedance of the cable connecting the inverter to the motor.

It is known that a DC/AC converter can be considered, at the supply-bus side, as a generator of harmonic currents, injected from the point A (Fig. 1) towards the network. These harmonic currents cause harmonic voltage drops along the line impedance Z_l, distorting the voltage at bus, B, and, thus, the supply voltage of every load connected to B. The extent of distortion is related to the ratio between the distorting load power and the short-circuit power of the equivalent network seen by B, so that even small power distorting loads can affect significantly the bus voltage if the line short-circuit power is low [1, 26-28].

Supply-bus voltage distortion can be further on magnified by the parallel resonances, which are not uncommon in electrical power networks having power-factor compensation capacitors. An example of a distorted voltage waveform recorded in an electrical plant is reported in Fig. 2. In this case, a parallel resonance close to 5^{th} harmonic occurred between capacitive and inductive equivalent impedances, so that the amplitude of harmonic components near the resonance frequency is comparable with the fundamental one. It is noteworthy that parallel resonances can commonly

occur in frequency ranges typical of those of the harmonic currents of noticeable amplitude, generated by converters, i.e. between the 5^{th} and 21^{st} harmonic order.

In addition to the AC-supply side harmonics, the DC/AC converter generates impulsive voltage waves, whose characteristics depend on the switching technique, the motor design, the length of the cable connecting the ASD with the motor [14, 17, 19, 21, 29, 30]. For example, a typical waveform generated by a PWM inverter with MOS-FET or IGBT technology at the motor terminals is reported in Fig. 3. The voltage is modulated according to sinusoidal law, by square pulses at high frequency (up to 50 kHz) with very high slew rate (up to 50 kV/us), so that high order harmonics only, related to the switching frequency, are present in the supply network. Very large spikes, even two times larger than the square-wave amplitude, as well as ringings in the correspondence of rise and fall fronts could be observed at the motor terminals, even if the inverter generates purely-square pulses. As mentioned above, the magnitude of these overshoots depends on the length of the cable connecting inverter and motor, through the impedance mismatches between inverter, cable and motor [29, 30]. The overshoot amplitude is related also to the rise time of the pulsed supply: the smaller the rise time, the larger the overshoot for a fixed cable length. Another problem is that these impulses will give rise to voltage potential distributions along the motor coils that, due to the high frequency content, tend to concentrate the maximum voltage drops on the first turns of the windings. If, due to random winding, the first and the last winding of a coil are in contact, the wire insulation will experience an electric field much larger than that expected under 50 Hz AC supply voltage. Hencefrom, and in combination with the voltage overshoots, accelerated insulation aging can be promoted. Even the degradation mechanism can change, since PD on the insulation surface (or in insulation cavities) can be triggered due to uneven potential distribution and overshoots. These PD would have not been expected according to the design, or have much larger amplitude and repetition rate with respect to the design conditions.

Contrarily to the sinusoidal case, where only one parameter, e.g. the RMS or peak value, is able to identify the voltage stress, the distorted regime requires more complex stress definitions, since infinite waveforms may have, for example, the same RMS but different shape or peak values. Appropriate parameters, characterizing the distorted voltage waveform, are, thus, needed in order to correlate the distorted waveform stress with the aging acceleration process. In [11, 12] it is shown that RMS and peak voltage, shape and steepness of the waveform can be used successfully for this purpose.

The next Section will provide the results of accelerated life tests performed on low-voltage self-healing capacitors and samples of motor wires, i.e. twisted pairs, subjected to AC-supply voltage distortion and ASD output voltage distortion, respectively. The discussion will point out those

parameters useful to identify the aging stress under voltage distortion and the correlation of distortion with accelerated aging.

3 Effect of Voltage Distortion on Insulation Accelerated Aging

3.1 Low Frequency Harmonics on self-healing capacitors

Multistress life tests were performed on self-healing capacitors with different combinations of harmonics and temperature levels, according to a so-called “screening experiment” of the Design of Experiment (DOE) procedure [31, 32].

In order to understand which features of the voltage waveform could prevail in promoting degradation acceleration, three shape parameters were defined [11, 12]:

$$K_f = \frac{\omega_1}{\omega_0}\sqrt{\sum_{h=1}^{N} h^2 \alpha_h^2} \quad (1)$$

$$K_P = \frac{V_P}{V_{1P}^*} \quad (2)$$

$$K_{rms} = \frac{V_{rms}}{V_{1rms}^*} \quad (3)$$

where V_1^* is the reference voltage (e.g. the rated capacitor 50 Hz voltage: V_{1rms}^* = 250 V, $V_{1P}^* = \sqrt{2} \cdot 250$ V), V_P and V_{rms} are peak and rms value of the considered waveform; N is the amount of harmonic components of noticeable amplitude contained in the voltage waveform, ω_1 is the angular frequency of the fundamental component, ω_0 = 314 rad s-1 is the angular frequency of the reference 50 Hz sinusoid, h is the harmonic order, $\alpha_h = V_h/V_1$.

It is noteworthy that the three parameters thus defined tend to 1 for a purely-sinusoidal supply-frequency (50 or 60 Hz) waveform.

The first coefficient is proportional to the RMS derivative of voltage waveform, thus to voltage steepness or current, the others are related to peak and rms voltage values, respectively.

The system employed for life tests, sketched in Fig. 4, is fully automated and controlled by a Personal Computer. It can generate, under high voltage, any kind of waveform with harmonic

components up to 1000 Hz, which is a frequency large enough to investigate the effect of AC-power network distortion.

Several life tests were carried out on samples of five self-healing capacitors. In each test the waveform parameters defined in equations (1)-(3) were varied superimposing to the fundamental one or more harmonic components, with different phase shifting. Most of the tests were carried out considering the worst case, i.e. when the harmonic amplitudes sum to the fundamental arithmetically.

The life tests were performed at three levels of temperature, i.e. 20, 60 and 90 °C, in order to obtain information on the multistress behavior of the capacitors. Therefore, besides the voltage waveform parameters, another one, derived from temperature, was needed to take into account also thermal aging, T [33]:

$$T = 1/\Theta_0 - 1/\Theta \tag{4}$$

where $\Theta_0 = 293$ K is the reference (room) temperature and Θ is the test temperature.

During the tests, the inner temperature, loss factor (tanδ) and capacitance were continuously monitored. Having observed in all the tests a continuous capacitance decreases with aging time (due to self-healing effect), the time elapsed for 10% derating from the nominal value was considered as failure time. The life test results are summarized in Table 1, which provides the voltage waveform, the test temperature, the electrical stress parameters and the mean failure times (life) with their 95% confidence intervals.

In order to single out the parameter having the larger effect on aging acceleration, the failure times reported in Tab.1 were correlated statistically with the aging factors defined in (1)-(4) by means of multivariate regression techniques [12]. The Main Effect Plot (MEP) of Fig. 5 shows the effect on failure times of the four considered aging factors. The lines represent the estimated effect of each factor: the higher the slope, the larger the effect on life of the relevant factor. In the case here considered it can be argued that the prevailing aging factor is the peak voltage K_P, followed, in descending order of importance, by rms voltage (K_{rms}), thermal stress (T) and voltage slope (K_f).

Regarding the thermal stress increase due to harmonic currents it has been shown in [34] that the harmonic currents constitute a secondary aging effect: it should be reminded, in fact, that K_f is related also to the rms current which flows through the capacitor and it is the least significant factor for aging, among those here considered. A thermal model is presented in [34], which provides the relationship among the rise of joule losses on the capacitor plates and heads, dielectric losses and temperature increase. It is shown that only for very large distortion levels (K_f>20) joule losses are not negligible with respect to dielectric losses and the temperature increase is, in the worst case,

about 10-15 °C. This variation is able to cause halving of life (see, e.g., [33, 35]), while even small K_P variations can cause failure time reduction of ten times or more [33, 34]. The temperature rise during a life test in a capacitor subjected to supply voltage indicated as sample #1 in Table 1 is reported in Fig. 6. Figure 6A shows the temperature behavior in the first 7h, with a rapid rise, the achievement of steady conditions at about 26°C, then again a steep increase. The weak temperature rise in the capacitor with respect to room temperature can be attributed to ohm and dielectric losses due to current and voltage distortion (in agreement with [34]). On the contrary, the considerable increase of temperature starting from 4.5h can be associated more to electrical features, i.e. inception of significant PD activity at capacitor heads and self-healing discharges, than to Joule or dielectric losses. The PD activity causes a rapid and large temperature growth, which can affect considerably degradation and stops once the capacitor tapes interested by PD are detached from the heads due to temperature and mechanical effects. This mechanism can explain the rapid temperature rise and falls in Fig. 6B (till the end-point used to determine the failure time), and, at the very end, capacitor breakdown. Hence, it can be concluded that capacitors can actually break due to thermal effects, but these effects can be activated by the harmonic overvoltage, rather than by harmonic currents.

These results confirm further on that, among the factors reported above describing electrical aging, the peak voltage is the main cause of capacitor insulation degradation.

On the basis of this approach and of the results of correlation algorithms, a life model can be provided, involving all the significant aging factors:

$$\ln t_F = \ln t_{F0} - n_f \ln K_f - n_P \ln K_P - n_{rms} \ln K_{rms} - hT \qquad (5)$$

where, for the specific capacitors tested, the values of the coefficients are: t_{F0}=72500 h; n_f =0.56; n_P =6.2; n_{rms} =1.8; h=1552 K.

A simple probabilistic investigation can be carried out in order to quantify the loss of reliability of capacitors as a function of peak amplification (K_P). For this purpose, the two-parameter Weibull probability distribution, which is mostly used to process data from electro-thermal life tests on solid insulation, can be employed [33]:

$$F(t_F) = 1 - \exp\left[-\left(\frac{t_F}{\alpha}\right)^{\beta} \right] \qquad (6)$$

where t_F is the failure time for a given probability $F(t_F)$, α is the scale parameter, i.e. the failure time corresponding to probability 63.2% and β is the shape parameter. The generalization of the failure time statistics can be obtained substituting in (6) α with t_F from expression (5). As a first

approximation, we can consider only the predominant factor K_P, so that the simplified model derived from (5) and (6) is:

$$F(t_F, K_P) = 1 - \exp\left[-\left(\frac{t_F}{t_{F0} K_P^{-n}}\right)^{\beta} \right] = 1 - \exp\left[-\left(\frac{t_F}{t_{F0}} K_P^{n}\right)^{\beta} \right] \quad (7)$$

The application of eq. (7) to the tested capacitors provides the plot of Fig. 7 (the values of t_{F0}, n and β are: t_{F0} = 66000 h, n = 8.5, β =1). Each curve represents the failure probability vs. aging time at different K_P values. It can be observed that the failure probability increases considerably with K_P. The effect of K_P on reliability reduction may be singled out better by Fig. 8, which shows the behavior of the cumulative failure probability corresponding to a life of sixth months (t_F = 4380 h) as function of the peak amplification. As can be seen, the failure probability increases steeply with K_P: for example, the probability of failure becomes about 50% with peak amplification of 30%, while it is only 6% with K_P =1.

Even if largely approximate, a model like that provided by eq. (7) is useful to infer the reliability of insulation systems connected to a distorted power network. However, more complex models can be achieved, taking into account also the random nature of harmonic amplitude (see e.g. [36]).

3.2 High Frequency Harmonics on twisted pairs

When a step-fronted voltage waveform is applied to the motor terminals, the first windings filter the signal, so that its slew-rate and magnitude decreases going to the end of the winding. Therefore, a pulse-like potential drop arises between the first and the last coil windings, whose amplitude increases with the slew rate of the PWM supply. If the winding is random wounded, as often occurs in low voltage AC-motors, the first coils may be adjacent to the last ones. In this way, the turn-to-turn insulation is stressed by bipolar pulses that could reach the amplitude of several hundred volt [29, 30]. The turn-to-ground insulation is stressed by a bipolar square wave as well, while the phase-to-phase voltage is typically unipolar (it is constituted by a series of pulses, modulated with a sinusoidal law, which reverse their polarity every T/2, where 1/T is the fundamental frequency of the output voltage [24]).

As mentioned before, standard electrical machine insulation, imide-amide based, suffers largely for PWM supply, while it withstands well 50-60 Hz sinusoidal voltage. In order to understand this behavior, life tests were carried out on four materials used for electrical machine windings: one standard (#A) and three belonging to the category of the so-called “corona resistant”, designed for ASD (#B, #C, #D). The insulation of #B, #C, #D is filled by inorganic (metallic) additives, with the

purpose of improving endurance to PD insulation erosion. Samples of 5 specimens were used for each life test. The specimens were realized by two enameled wires (l =120 mm, Φ =1 mm, mean insulation thickness = 0.13 mm), wound in a standardized way as a twisted pair [37].

The test apparatus is composed by a low-voltage square-wave generator, PC-controlled via IEEE488 bus. The output signal is then amplified in power and voltage by means of a static high-voltage switch, built by MOS-FET technology. This component can reach, in a push-pull configuration, a slew rate up to 100 kV/μs and voltage amplitude of ±5 kV, providing both unipolar and bipolar square-wave. The voltage waveform is monitored by an oscilloscope through a compensated HV probe. The maximum capacitance load which can be connected to the generator is about 150 pF, which allows simultaneous testing of up to 5 specimens of the twisted pair type (about 25 pF each).

First, life tests were performed on the four materials considered by a 50 Hz sinusoidal waveform, at three voltage levels, with the specimens either kept in air or immersed in silicon oil, in order to promote aging in the presence and in the absence of PD, respectively. The purpose was, indeed, to single out the effect of PD on aging acceleration. Preliminary measurements of Partial Discharge Inception Voltage (PDIV) were performed on the twisted pairs both in oil and in air, in order to establish test voltage levels above and below PDIV for life tests in air and in oil, respectively. The PDIV measured at 50 Hz, sinusoidal wave, was 9000 V and 700 V for twisted pairs immersed in silicon oil and in air, respectively.

Then, life tests at 10 kHz under both sinusoidal and square-waves (the latter unipolar or bipolar), were carried out in air. Three or four voltage levels were applied, while other square-wave parameters were maintained constant (duty cycle 50%, rise time 0.75 kV/us), with the purpose to achieve information on the on the effect of voltage peak and frequency on acceleration of insulation aging in the presence of partial discharges, for standard and corona resistant materials. The effect of rate of voltage rise (slew rate) and duty cycle, already partially discussed in literature [15, 16, 38], are still under investigation through a DOE procedure. As for the 50 Hz life tests, PDIV measurements were performed under high frequency supply (sinusoidal and square wave), in order to choose the voltage levels for the life tests to be performed above PDIV. Figure 9 shows PD signals measured by a digital oscilloscope on a twisted pair supplied by unipolar square-wave voltage (2.0 kV peak-to-peak (pp), slew rate = 0.75 kV/us, duty cycle = 50%). For this kind of measurement the PD signal coming from the specimen is appropriately filtered in order to separate the noise due to switching frequency from the useful PD signal. We can observe in Fig. 9 that the maximum PD activity is reached just after the step-front, with a very short time lag.

For each life test, the failure times were statistically processed by the 2-parameter Weibull distribution (eq. (6)).

An Inverse Power Model (IPM) was used to fit the 63,2% failure times at the different test stress levels. In a log-log plot, this model provides a straight line with slope inversely proportional to the Voltage Endurance Coefficient, *n* (VEC) [33]:

$$t_F = kV^{-n} \tag{8}$$

where V is the peak voltage, k and n are the parameters of the model. Figures 10-12 report the results of life tests (and the relevant regression lines) at 50 Hz, in oil and/or in air, and at high frequency, only in air, with sinusoidal waveform. As can be seen, experimental data fits to a linear log-log relationship mostly with very good approximation.

The results of life tests at 50 Hz and 10 kHz sinusoidal in air and in oil for material #A (Fig. 10) emphasize the effect of frequency increase on aging acceleration of conventional insulation, both in the presence and in the absence of PD activity. Looking at the life lines, it comes out that the failure times and the VEC relevant to the life tests performed in silicon oil are larger than those derived from tests in air, so that the electric stress seems to accelerate aging much more in air (where PD are active) than in oil. Of course, failure occurs also in the absence of PD but at longer times. Moreover, it can be observed that the failure times for the life tests in air at 10 kHz are several order of magnitude shorter than at 50 Hz. The increase of frequency to 10 kHz causes even larger differences in failure times between the specimens aged in oil and in air with respect to 50 Hz supply, further on confirming the dramatic effect of PD for aging acceleration (PD, in fact, will significantly increase with frequency [39-40]). However it is noteworthy that frequency-accelerated aging is considerable even in the absence of PD (tests in silicon oil), and the endurance coefficient is reduced noticeably (VEC decreases from 11.7 to 8.7).

The four different materials tested are compared, in order to evaluate their behavior with different kinds of supply waveforms, in Figures 11-14.

Figure 11 reports the life test results obtained in air under 50 Hz sinusoidal voltage for the four materials #A to #D. It is interesting to observe that materials #B e #D present significantly shorter life than #A, the reference material, at the same voltage level, while #C shows the longest life times and best endurance coefficient (VEC=10.6). Therefore, some corona resistant materials, manufactured specifically for motors supplied by PWM inverters, show a worse performance at 50 Hz than the standard insulating material, #A.

The behavior of these insulating materials is completely different, however, when the supply frequency increases. The data plotted in Fig. 12 and relevant to life test results under 10 kHz sinusoidal supply, performed in air, show that materials #B and #C have better endurance than #A, contrarily to what happens at 50 Hz. In fact, the life of #C may be at least 100 times that of #A at the same voltage. In this case, #D and #A have close lives, so that #D seems to have bad performance both at 50 Hz and at high frequency. It is noteworthy that the endurance coefficient of #C is considerably high (VEC=12.8), as it occurs at 50 Hz.

The strong dependence on frequency, displayed by a material as #B with respect to #A, might be explained through the effect of space-charges and polarization losses. At 50 Hz #B, doped with inorganic oxides and, thus, affected by an increased amount of internal interfaces, may accumulate much more space charge and present larger dielectric losses than #A, which can worsen life performance of such material. On the contrary, at 10 kHz space-charge accumulation, as well as interfacial and dipolar polarization losses, could be significantly reduced (literature shows evidence of a decrease of space charge build up as frequency increases [41]), while PD (corona) activity is largely increased with respect to 50 Hz. Hence, corona resistant materials may last longer than the standard one. Similar results are shown in [42], where a relationship between PDIV decrease and space charge build up is hypothesized. Corona resistant materials, in fact, exhibit a lower PDIV, even if they show a better PD endurance.

The effect of 10 kHz unipolar square and bipolar sinusoidal waveforms for the four tested materials is summarized in Figure 13, which collects the whole data set obtained by the life tests discussed above, as function of rms voltage. It is noteworthy that 10 kHz sinusoidal (bipolar) life tests provide failure times one order of magnitude shorter, at least, than those provided by the unipolar squarewave performed at the same rms. Partial discharges are much more active, in fact, with bipolar rather than unipolar supply voltage. However, if the data collected in Fig. 13 are plotted as function of peak-to-peak voltage it can be observed that all the high frequency data fits quite well the same straight line, for each material, independently of the voltage waveshape. This confirms that the peak-to-peak voltage is the most significant feature of the voltage waveform which causes the acceleration of the degradation process independently of the voltage waveshape. According to literature, [16], it can be expected that the pulse slew rate will affect significantly aging acceleration only at very high values (this aspect, as well as the influence of the duty cycle, is under investigation). The acceleration effect of frequency plays also a fundamental role, particularly for aging under an intense PD (corona) regime [18]. It is noteworthy that the frequency increase does not reflect in the same way on the different tested materials, being capable to accelerate aging of materials as #A and #D, but also able to improve the life performance of #B and #C.

4 Conclusions

The analysis here carried out points out that the voltage peak is the prevailing factor accelerating degradation of insulation systems fed by both low frequency and high frequency harmonics. The other factors are voltage rms, shape and thermal stress for low frequency harmonics, while frequency plays a prevailing role for high frequency harmonics. Regarding the latter case, the investigation of the effects of sinusoidal and square waveforms on standard and corona resistant coating materials subjected to life tests under partial discharges, reveals that life reduction is considerably larger with bipolar waveforms, for a given rms value, with respect to unipolar pulses. However, if the peak-to-peak voltage is considered, the failure times do not differ considerably, at a given frequency, from bipolar sinusoidal to unipolar square waveforms. The different materials tested do not provide consistent information regarding the capability to withstand PD aging at different frequencies and with different waveforms. Not all the tested corona resistant materials, in fact behave well at high and at low frequency, which could be related with the different role played by space charge accumulation as function of frequency.

References

[1] IEEE 519, *Recommended Practices and Requirements for Harmonic Control in Electric Power Systems*, December 1992.

[2] IEC 1000-3-2, *Electromagnetic compatibility (EMC) – Part 3: Limits – Section 2: Limits for Harmonic Current Emission*, First Edition, March 1995.

[3] IEC 61 642, *Industrial AC Networks Affected by Harmonics - Application of Filters and Shunt Capacitors*, 1997.

[4] IEEE Task Forces, "The Effect of Power System Harmonics on Power System Equipment and Loads", IEEE Trans. on Power App. Sist., Vol. 104, n. 9, pp. 2555-2563, September 1985.

[5] IEEE Task Force on the Effects of Harmonics on Equipments, "Effects of Harmonics on Equipment", IEEE Trans. on Power Del., Vol. 8, n. 2, pp. 672-680, April 1993.

[6] E.F. Fuchs, D.J. Roesler and K.P. Kovacs, "Aging of electrical appliances due to harmonics of the power system's voltage", IEEE Trans. on Power Del., Vol. 1, n. 3, pp. 301-307, July 1986.

[7] T.S. Key and J.-S. Lai, "Costs and Benefits of Harmonic Current Reduction for Switch-mode Power Supplies in a Commercial Office Building", IEEE Trans. on Ind. Appl., Vol. 32, n. 5, pp. 1017-1024, October 1996.

[8] G. Carpinelli, P. Caramia, E. Di Vito, A. Losi and P. Verde, "Probabilistic Evaluation of the Economical Damage due to Harmonic Losses in Industrial Energy System", IEEE Trans. on Power Del., pp. 1021-1031, April 1996.

[9] I. Ghinello, G. Mazzanti, G.C. Montanari, D. Fabiani and A. Cavallini, "An Investigation of the Endurance of Capacitors Supplied by Nonsinusoidal Voltage", IEEE CEIDP, pp. 723-727, Atlanta, GA (USA), October 1998.

[10] A. Cavallini, I. Ghinello, G. Mazzanti and G.C. Montanari, "Considerations on the Life Performances and Installation Practice of Shunt Capacitors in the Presence of Harmonics Generated by AC/DC Converters", IEEE Trans. on Power Del., Vol. 14, N. 1, pp. 227-234, January 1999.

[11] G.C. Montanari and D. Fabiani, "Searching for the Factors which Affect Self-healing Capacitor Degradation under Non-sinusoidal Voltage", IEEE Trans. on Diel. El. Ins., Vol. 6, N. 3, pp. 319-325, June 1999.

[12] G.C. Montanari and D. Fabiani, "The Effect of Non-sinusoidal Voltage on Intrinsic Aging of Cable and Capacitor Insulating Materials", IEEE Trans. on Diel. El. Ins., Vol. 6, N. 6, pp. 798-802, December 1999.

[13] S.B. Warder, F. Friedlander and A.N. Arman, "The Influence of Rectifier Harmonics in a System on the Dielectric Stability of 33-kV Cables", CIGRE, paper no.1025, 1950

[14] A.H. Bonnett and G.C. Soukup, "Cause and Analysis of Stator Rotor Failures in Three-Phase Squirrel-Cage Induction Motors", IEEE Trans. on Ind. Appl., Vol.28, N.4, pp.921-937, July 1992.

[15] W. Yin, K. Bultemeier, D. Barta and D. Floryan, "Critical Factors for Early Failure of magnet Wires in Inverted-Fed Motors", IEEE CEIDP, pp.258-261, San Francisco, CA (USA), October 1995.

[16] Weijun Yin, " Failure Mechanism of Winding Insulation in Inverter-Fed Motors", IEEE El. Ins. Magazine, Vol. 13, N. 6, pp.18-23, November 1997.

[17] M. Kaufhold, G. Borner, M. Eberhardt and J. Speck, " Failure Mechanism of Low Voltage Electric Machines Fed by Pulse-Controlled Inverters", IEEE El. Ins. Magazine, Vol. 12, N. 5, pp.9-15, September 1996.

[18] K. Bauer, M. Kaufhold and H. Wang, "High Voltage Motor Winding Insulation for High Power Adjustable Speed Drives Fed by IGBT-Converter", 8th BEAMA '98, pp.257-263, Harrogate, UK, May 1998.

[19] E. Persson, "Transient Effects in Application of PWM Inverters to Induction Motors", IEEE Trans. on Ind. Appl., Vol. 28, N. 5, pp.1095-1101, September 1992.

[20] G.C. Stone, R.G. van Heeswijk and R. Bartnikas, "Investigation of the Effect of Repetitive Voltage Surges on Epoxy Insulation", IEEE Trans. on Energy Conv., Vol. 7, N. 4, pp. 754-759, December 1992.

[21] J.A. Oliver and G.C. Stone, “Implications for the application of adjustable speed drive electronics to motor stator winding insulation”, IEEE El. Ins. Magazine, Vol. 11, N. 4, pp.32-36, July 1995.

[22] V. Divljankovic, J. Kline, J. Akers and K. Theis, "Multifactor Aging of Electrical Machines Energized by Standard PWM Drives", IEEE CEIDP, pp.808-812, San Francisco, CA (USA), October 1996.

[23] J.P. Bellomo, P. Castelan and T. Lebey, "The Effect of Pulsed Voltages on Dielectric Material Properties", IEEE Trans on Diel. and El. Ins., Vol. 6, N. 1, pp.20-26, February 1999.

[24] G.C. Montanari, D. Fabiani and A. Contin, “Aging Investigation of Turn Insulation under Fast Repetitive Pulse Voltage with or without Partial Discharges”, CWIEME’99, pp. 88-96, Berlin, Germany, June 1999.

[25] A. Cavallini, D. Fabiani, G. Mazzanti, G.C. Montanari and A. Contin “Voltage Endurance of Electrical Components Supplied by Distorted Voltage Waveforms”, IEEE ISEI, pp.73-76, Anaheim, CA (USA), April 2000.

[26] A. Cavallini, M. Loggini and G.C. Montanari, "Comparison of Approximate Methods for Estimate Harmonic Currents Injected by AC/DC Converters", IEEE Trans. on Ind. Electronics, Vol. 41, N. 2, pp. 256-262, April 1994.

[27] A. Mansoor, W.M. Grady, R.S. Thallam, M.T. Doyle, S.D. Krein and M.J. Samotyj, “Effect of Supply Voltage Harmonics on the Input Current of Single-phase Diode Bridge Rectifier Loads”, IEEE Trans. on Power Del., Vol. 10, N. 3, pp. 1416-1422, July 1995.

[28] E. W. Kimbark, *Direct Current Transmission*, Wiley, New York, NY (USA),1971.

[29] J.P. Bellomo, T .Lebey, J. M. Oraison and F. Peltier, "Characterization of Voltage Shapes Acting on the Insulation of Rotating Machines Supplied by Inverters", IEEE ICPADM, pp.792-795, Brisbane, Australia, July 1994.

[30] J.P. Bellomo, *Etude des Consequences des Nouvelles Formes de Commande sur les Materiaux de l'Isolation Statorique*, Ph.D Thesis, Universitè Paul Sabatier, Toulouse, France, 1996.

[31] D.C. Montgomery, *Design and Analysis of Experiments*, Wiley, New York, NY (USA),1997.

[32] STATGRAPHICS R.3.0 for Windows 95, Manugistics Inc. 1997.

[33] L. Simoni, *Fundamentals of Endurance of Electrical Insulating Materials*, CLUEB, Bologna, Italy, 1983.

[34] A. Cavallini, D. Fabiani, G. Mazzanti, and G.C. Montanari “Models for Degradation of Self-healing Capacitors Operating under Voltage Distortion and Temperature”, IEEE ICPADM, pp. 108-111, Xian, China, June 2000.

[35] G.C. Montanari and F. J. Lebok," Thermal Degradation of Electrical Insulating Materials and Thermokinetic Background", IEEE Trans on El. Ins., Vol. 25, N. 6, pp.1029-1036, December 1990.

[36] A. Cavallini, D. Fabiani, G. Mazzanti and G.C. Montanari "The Effect of Power System Harmonics on Cable Endurance: a Critical Review to IEEE Std. 519 Voltage Distortion Limits", IEEE IAS 35th Annual Meeting, pp.3172-3179, Rome, Italy, October 2000.

[37] ASTM Standard D1676, Standard Methods for Testing Film-Insulated Magnet Wire, Annual Book of ASTM Standards, Vol. 01.03, 1983.

[38] N. Foulon, J.P. Lucas, G. Barré, R. Mailfert and J. Enon, "Investigation of the Failure Mechanism of Insulation Subjected to Repetitive Fast Voltage Surges", IEEE EIC and EMCW, pp. 401-406, Rosemont, IL (USA), September 1997.

[39] G. C. Stone, S. Campbell and S. Tetreault, "Inverter-Fed Drives: Which Motor Stators are at Risk?", IEEE Ind. Appl. Magazine, Vol. 6, N. 5, pp. 17-22, October 2000.

[40] W. Pfeiffer and M. Paede, "About the Influence of the Frequency on the Partial Discharge Characteristics of Enamelled Wires", IEEE EIC and EMCW, pp. 485-488, Cincinnati, OH (USA), October 1999.

[41] T. Takada, "Acoustic and Optical Methods for Measuring Electric Charge Distribution in Dielectrics" ", IEEE Trans. on Diel. El. Ins., Vol. 6, N. 5, pp. 519-547, October 1999.

[42] C. Hudon, N. Amyot and D. Jean, "Long Term Behavior of Corona Resistant Insulation Compared to Standard Insulation of Magnet Wire", IEEE ISEI, pp. 13-16, Anaheim, CA (USA), April 2000.

Authors' Biography:

Davide Fabiani was born in Forlì, Italy, on 7th January, 1972. He received the M.Sc. in Electrical Engineering (cum laude) in 1997 from the Faculty of Engineering, University of Bologna. After a one-year fellowship provided by "Pirelli Cable & Systems", since November 1998 he has been a Ph. D. Student in Electrical Engineering at the Material Engineering & High Voltage Laboratory of the University of Bologna. Since 1998 he has been a student member of IEEE DEIS. His current research interests deal with aging investigation of insulating materials and diagnosis, particularly the effect of harmonic distortion on electrical equipments, e.g. cables, capacitors, electrical machines.

Gian Carlo Montanari was born in Bologna, Italy, on Nov. 11, 1955. He received his degrees in electrical engineering from the University of Bologna. In 1983 he became an assistant professor and in 1986, professor of electrical technology. He has worked since 1979 in the field of aging and endurance of insulating materials and systems. He is also engaged in the topics of harmonic compensation in electrical power systems, power electronics and statistics. He is an IEEE fellow, a member and convener of WG of IEC 15E, 98 and 33, as well as the Italian representative in CIGRE' SC15. He may be reached at the Department of Electrical Engineering, Viale Risorgimento 2, I-40136 Bologna, Italy. Tel.:+39-051.2093481. Fax: +39-051.2093470. E-mail: giancarlo.montanari@mail.ing.unibo.it.

Table 1: Summary of life test data and results: V_1, V_3, .., V_h are fundamental, 3rd ,…, hth harmonic components of test voltage waveform. Their rms value is 250 V. Voltage shape coefficients, K_f, K_P, K_{rms} and test temperatures, Θ_e, are reported. The mean failure times, $\bar{t}_F$, are given with their 95% confidence intervals. The superscripts °, π, φ indicate a phase shifting between fundamental and harmonic component of 0°, 180° and 111.5° respectively. $\Gamma = V_1+1/3V_3°+1/5V_5°+1/7V_7°$.

Sample #	Supply Voltage	Θ_e [°C]	V_{rms} [V]	V_p [V]	K_f	K_P	K_{rms}	$\bar{t}_F$ [h]
1	$V_1+2V_3{}^{\pi}$	20	560	1060	6.08	3.00	2.24	9.1 ± 2.4
2	$V_1+3V_3{}^{\pi}$	20	760	1414	9.06	4.00	3.04	0.3 ± 0.2
3	$2.24V_1$	20	560	792	1.00	2.24	2.24	115 ± 3.9
4	$V_1+1.5V_3{}^{\pi}$	20	450	884	4.61	2.50	1.80	22 ± 5.5
5	$V_1+2V_{11}{}^{\pi}$	20	560	1060	22.0	3.00	2.24	2.9 ± 2.4
6	$3V_1$	20	750	1060	1.00	3.00	3.00	14 ± 5.2
7	$V_1+2.4V_{11}{}^{\pi}$	20	650	1202	26.4	3.40	2.60	1.7 ± 0.6
8	$2.6V_1$	20	650	919	1.00	2.60	2.60	29 ± 1.4
9	$2.24V_3$	20	560	792	3.00	2.24	2.24	46 ± 31
10	$V_1+1.5V_{11}{}^{\pi}$	20	450	884	16.5	2.50	1.80	24 ± 13
11	$2.24V_{11}$	20	560	792	11.0	2.24	2.24	30 ± 12
12	$2V_1+1.14V_5{}^{\varphi}$	20	575	1060	3.02	3.00	2.30	10 ± 3
13	$3V_5$	20	750	1060	5.00	3.00	3.00	3.9 ± 1
14	$1.52(V_1+V_5°)$	20	537	1075	5.10	3.04	2.15	8.1 ± 1.2
15	$3V_1$	60	750	1060	1.00	3.00	3.00	5.6 ± 1.8
16	$2.24V_3$	60	560	792	3.00	2.24	2.24	23 ± 5.0
17	$2.24V_3$	90	560	792	3.00	2.24	2.24	16 ± 2.4
18	Γ	20	560	680	2.00	1.92	2.24	166 ± 15
19	Γ	60	560	680	2.00	1.92	2.24	142 ±12
20	$2.24V_1$	60	560	792	1.00	2.24	2.24	89± 8.2

Figure Captions:

Fig. 1: Example of an AC-power network with distorting and non-distorting loads.

Fig. 2: Example of voltage waveform recorded in an electrical plant, where 5^{th} harmonic is amplified by a parallel resonance.

Fig. 3: Typical voltage waveform at PWM-controlled motor terminals.

Fig. 4: Scheme of the system for life tests on self-healing capacitors. PC = personal computer; CT = current transformer, VT = voltage transformer.

Fig. 5: Main Effect Plot (MEP) obtained from the data of Table 1, reporting the estimated effect on logarithm of failure times of the four aging factors. Self-healing capacitors.

Fig. 6: Inner temperature behavior for a capacitor subjected to the voltage waveform #1 of Table 1: first 7 h (A) and whole test (B). Room temperature = 22°C.

Fig. 7: Failure probability vs. aging time for different K_P values. Self healing capacitors.

Fig. 8: Failure probability corresponding to life of sixth months as function of peak value amplification, K_P. Self healing capacitors.

Fig. 9: PD pulses measured for a twisted pair supplied by unipolar square-wave at 2.0 kV, 0.75 kV/μs of slew rate, 50% of duty cycle.

Fig. 10: Life test results of 50 Hz and 10 kHz sinusoidal supply in air and in oil for material #A. The life lines plotted according to eq. (8) are reported. The VEC is indicated for the life lines.

Fig. 11: Life test results of 50 Hz sinusoidal supply in air for all the four tested material. The life lines plotted according to eq. (8) are reported. The VEC is indicated for the life lines.

Fig. 12: Life test results of 10 kHz sinusoidal waveform in air for all the four tested material. The life lines plotted according to eq. (8) are reported. The VEC is indicated for the life lines.

Fig. 13: Summary plot in which all the data obtained from life tests on the four materials and the relevant life lines are reported as a function of rms voltage.

Fig. 14: The same of Fig. 13 plotted as function of peak-to-peak voltage.

Fig. 1

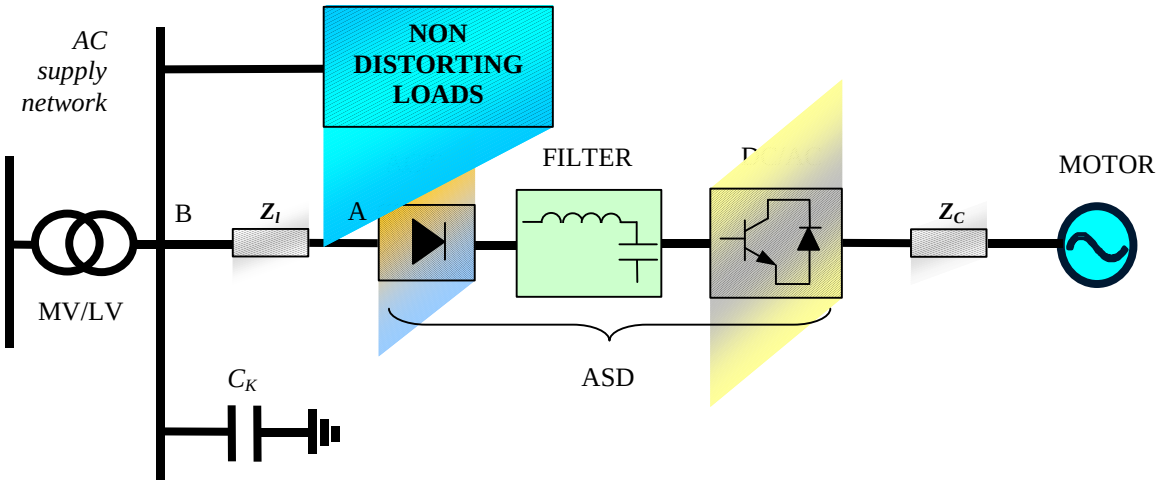
AC
supply
network
NON
DISTORTING
LOADS
FILTER
MOTOR
B
Z_l
A
Z_C
MV/LV
C_K
ASD

Fig. 2

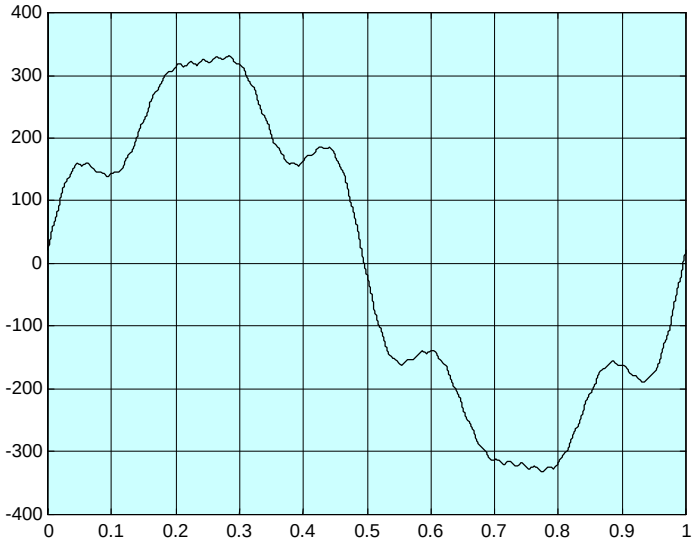
400
300
200
100
0
-100
-200
-300
-400
0
0.1
0.2
0.3
0.4
0.5
0.6
0.7
0.8
0.9
1

Fig. 3

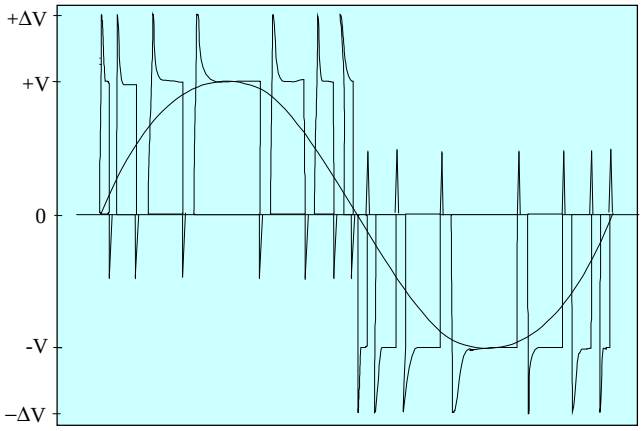
+ΔV
+V
0
-V
−ΔV

Fig. 4

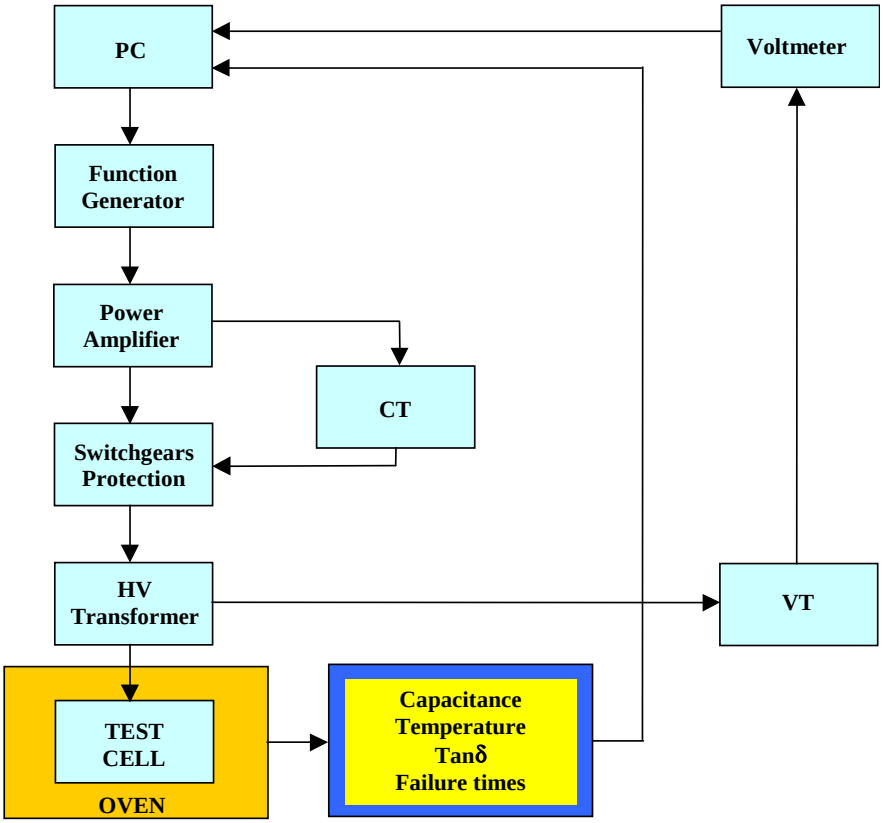
PC
Voltmeter
Function Generator
Power Amplifier
CT
Switchgears Protection
HV Transformer
VT
TEST CELL
OVEN
Capacitance
Temperature
Tanδ
Failure times

Fig. 5

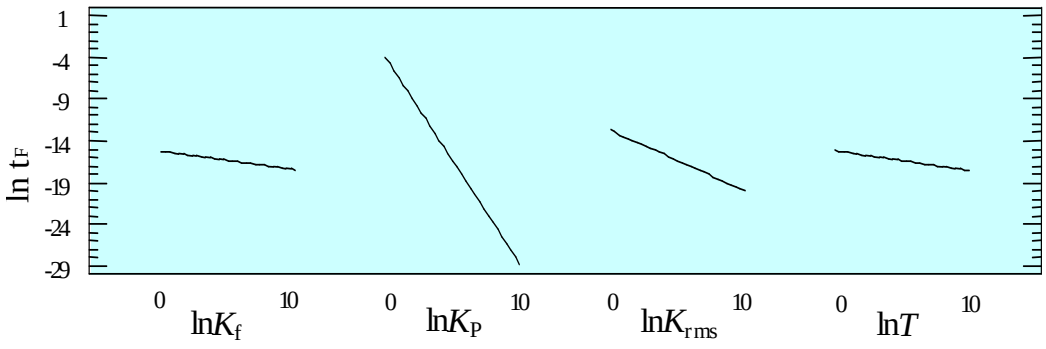
1
-4
-9
-14
-19
-24
-29
ln t_F
0
10
lnK_f
0
10
lnK_P
0
10
lnK_{rms}
0
10
ln$T$

Fig. 6A

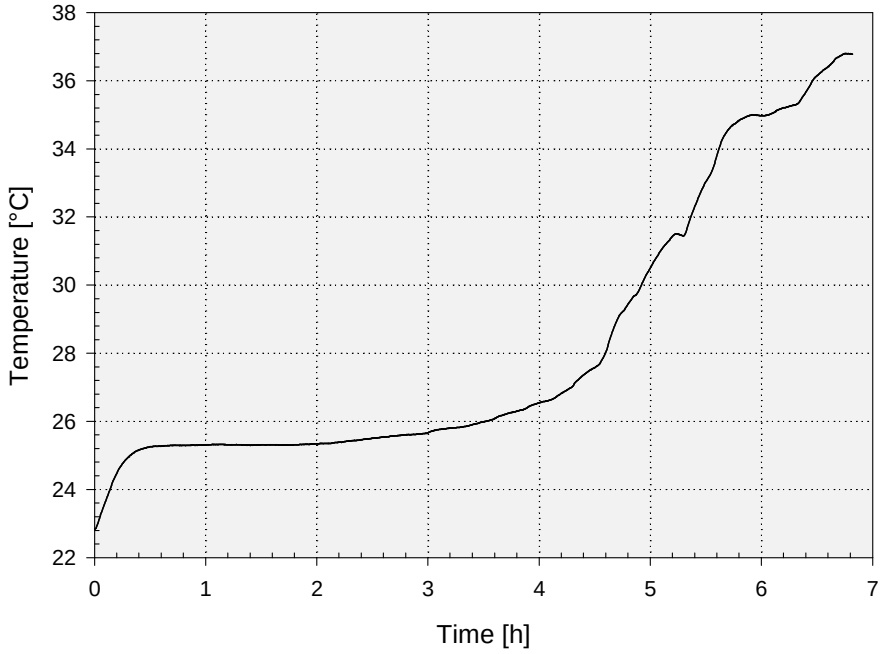
Temperature [°C]
38
36
34
32
30
28
26
24
22
0
1
2
3
4
5
6
7
Time [h]

Fig. 6B

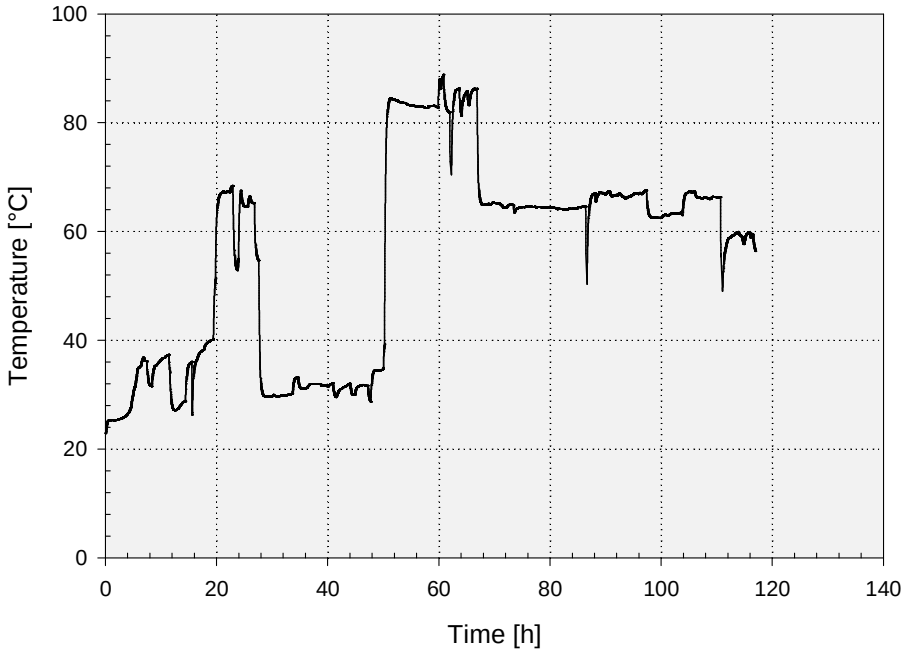
Temperature [°C]
100
80
60
40
20
0
0
20
40
60
80
100
120
140
Time [h]

Fig. 7

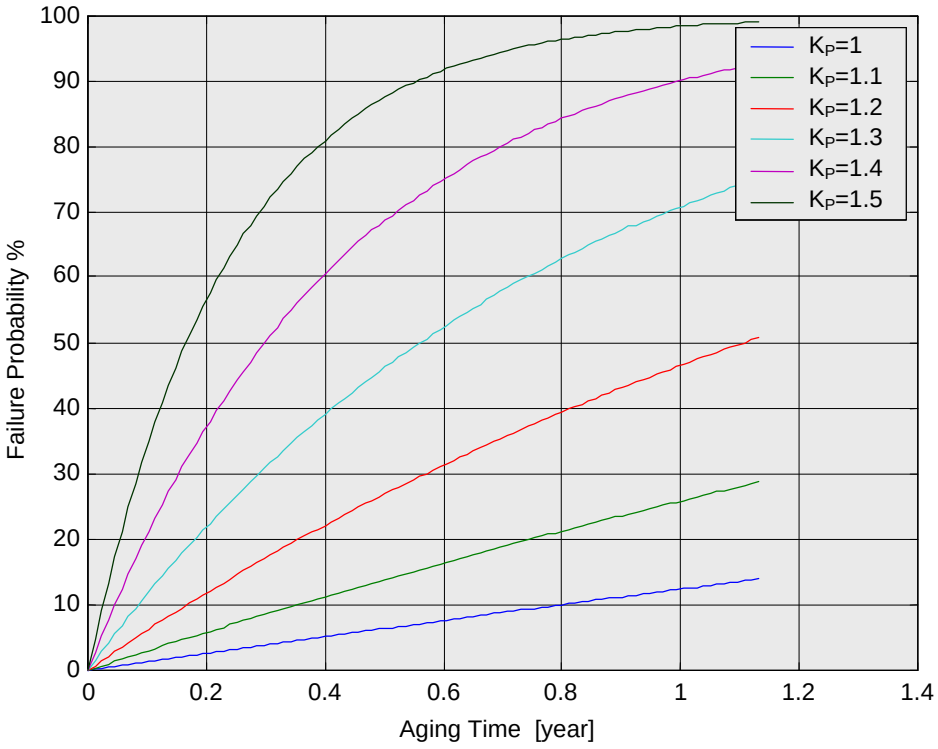
Failure Probability %
Aging Time [year]
KP=1
KP=1.1
KP=1.2
KP=1.3
KP=1.4
KP=1.5
0
10
20
30
40
50
60
70
80
90
100
0
0.2
0.4
0.6
0.8
1
1.2
1.4

Fig. 8

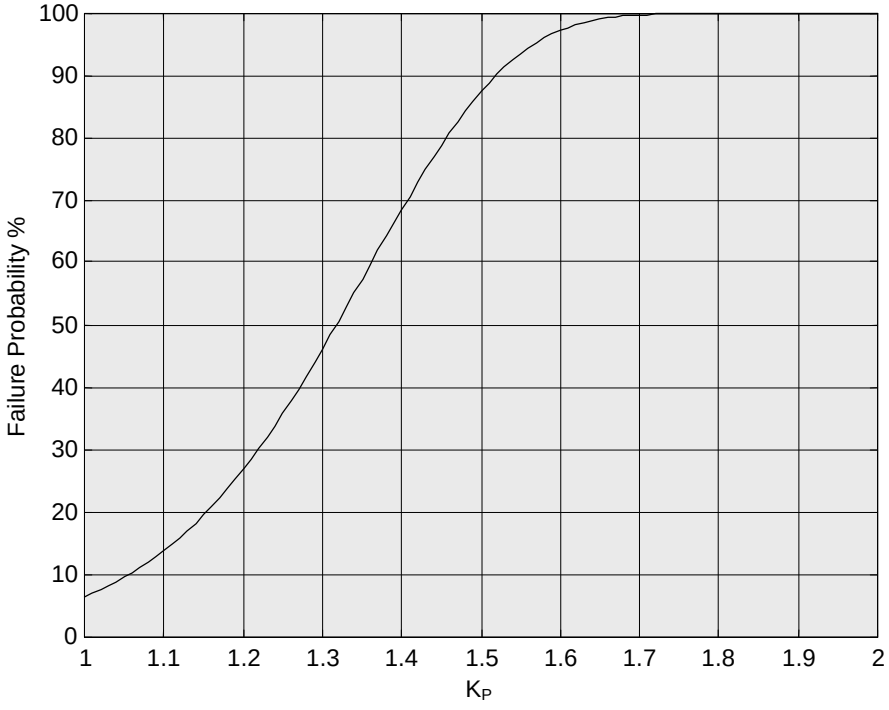
Failure Probability %
KP
0
10
20
30
40
50
60
70
80
90
100
1
1.1
1.2
1.3
1.4
1.5
1.6
1.7
1.8
1.9
2

Fig. 9

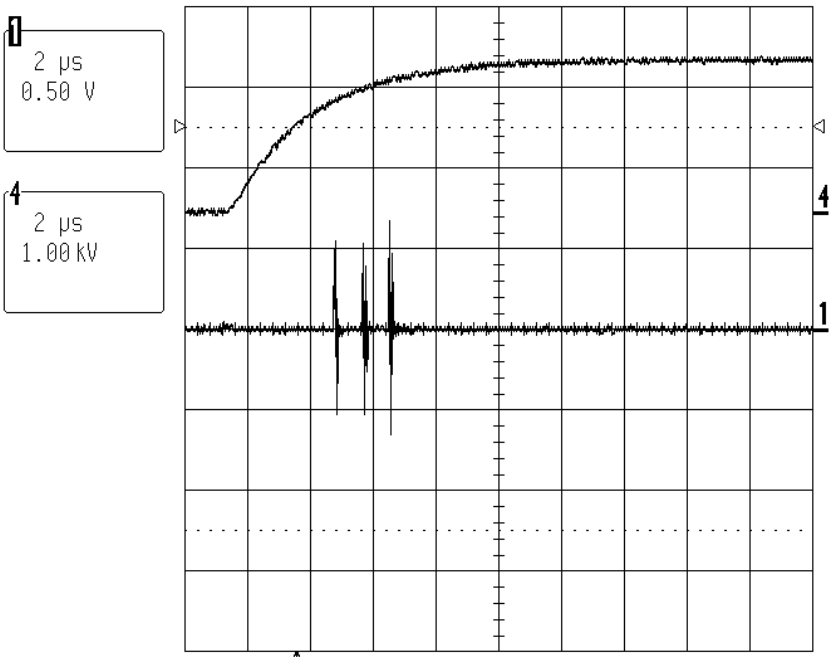
1
2 µs
0.50 V
4
2 µs
1.00 kV
4
1

Fig. 10

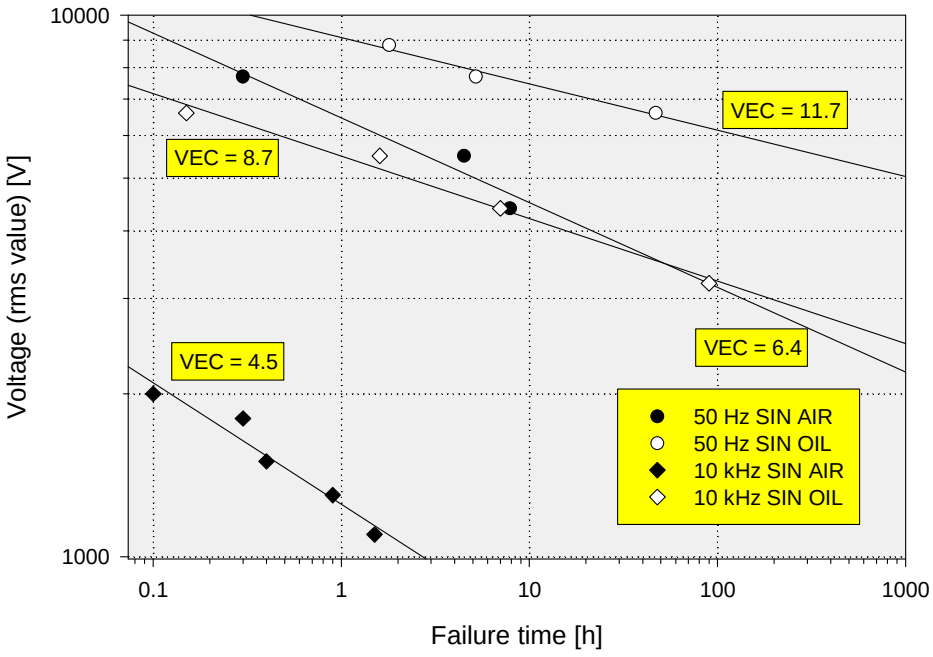
10000
1000
Voltage (rms value) [V]
0.1
1
10
100
1000
Failure time [h]
VEC = 11.7
VEC = 8.7
VEC = 6.4
VEC = 4.5
50 Hz SIN AIR
50 Hz SIN OIL
10 kHz SIN AIR
10 kHz SIN OIL

Fig. 11

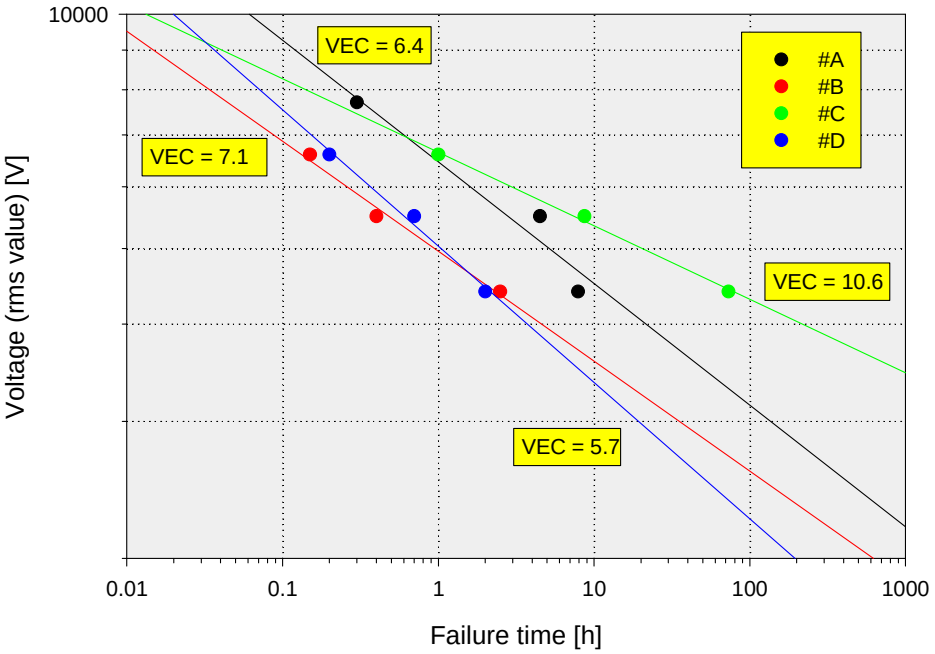
10000
VEC = 6.4
VEC = 7.1
VEC = 10.6
VEC = 5.7
#A
#B
#C
#D
Voltage (rms value) [V]
0.01
0.1
1
10
100
1000
Failure time [h]

Fig. 12

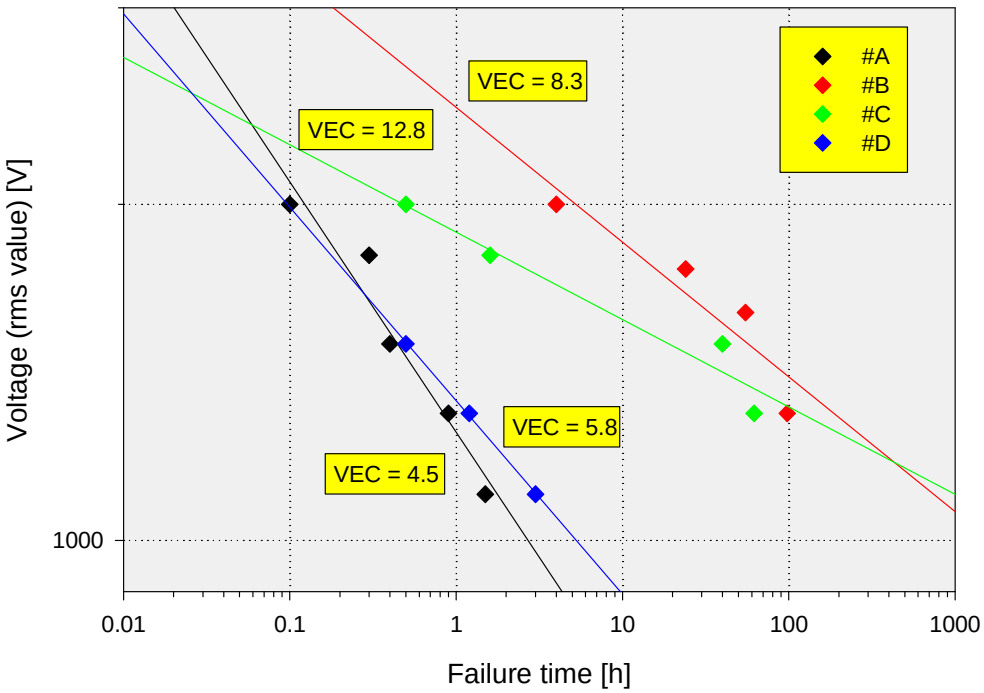
VEC = 8.3
VEC = 12.8
VEC = 5.8
VEC = 4.5
#A
#B
#C
#D
Voltage (rms value) [V]
1000
0.01
0.1
1
10
100
1000
Failure time [h]

Fig. 13

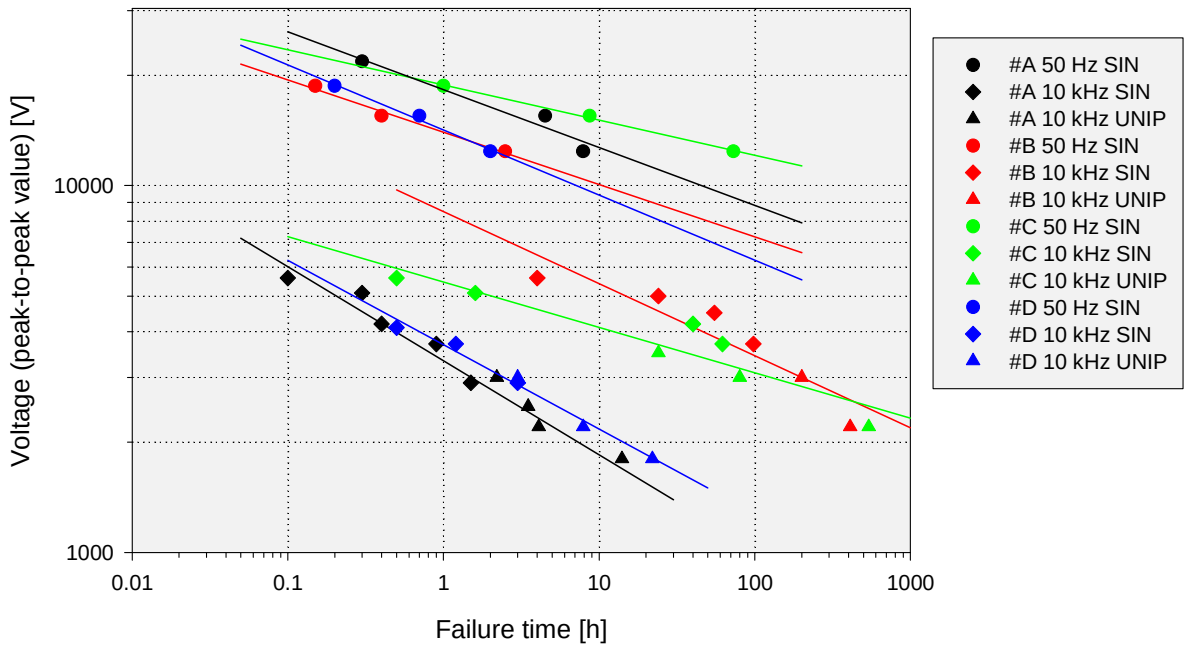
Voltage (peak-to-peak value) [V]
10000
1000
0.01
0.1
1
10
100
1000
Failure time [h]
#A 50 Hz SIN
#A 10 kHz SIN
#A 10 kHz UNIP
#B 50 Hz SIN
#B 10 kHz SIN
#B 10 kHz UNIP
#C 50 Hz SIN
#C 10 kHz SIN
#C 10 kHz UNIP
#D 50 Hz SIN
#D 10 kHz SIN
#D 10 kHz UNIP

Fig. 14

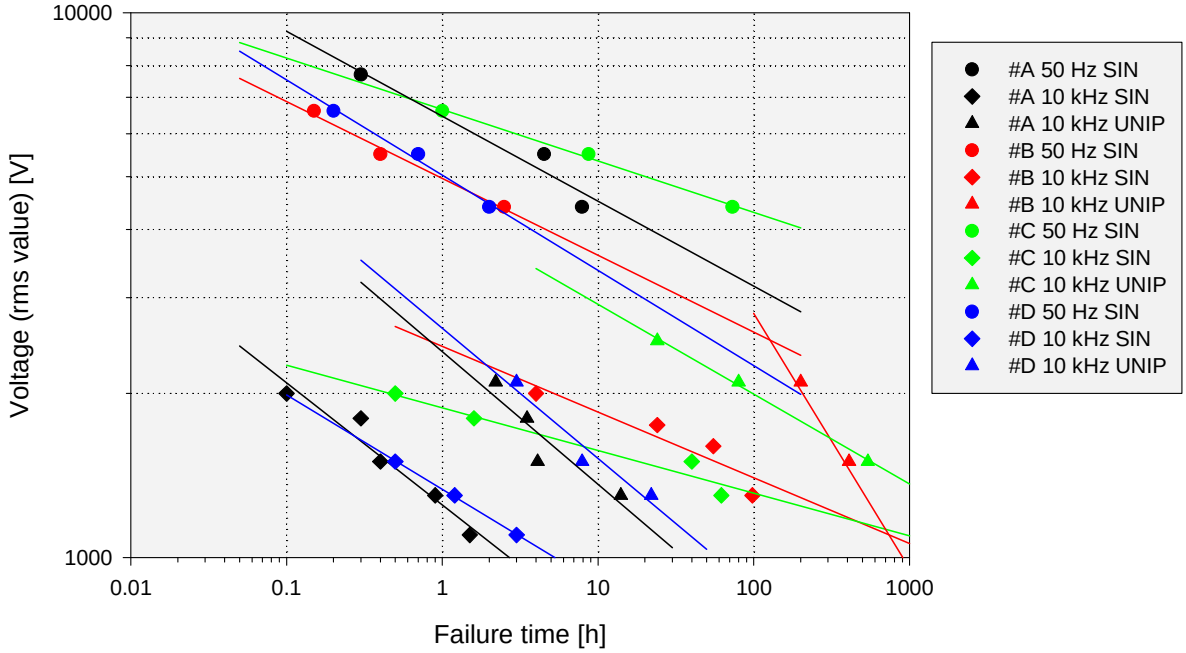
Voltage (rms value) [V]
10000
1000
0.01
0.1
1
10
100
1000
Failure time [h]
#A 50 Hz SIN
#A 10 kHz SIN
#A 10 kHz UNIP
#B 50 Hz SIN
#B 10 kHz SIN
#B 10 kHz UNIP
#C 50 Hz SIN
#C 10 kHz SIN
#C 10 kHz UNIP
#D 50 Hz SIN
#D 10 kHz SIN
#D 10 kHz UNIP